

# INVESTIGATION OF THE IMPLEMENTATION OF LEADER-FOLLOWER FORMATION CONTROL TO BIPEDAL LOCOMOTION

Djati Wibowo Djamari<sup>a</sup>, Ignatius Pulung Nurprasetio<sup>b\*</sup>, Fitri Endrasari<sup>a</sup>, Vania Katherine Mulia<sup>a</sup>

<sup>a</sup>Autonomous Systems Laboratory, Mechanical Engineering Study Program, Sampoerna University, Jakarta Selatan, Indonesia

<sup>b</sup>Faculty of Mechanical and Aerospace Engineering, Institut Teknologi Bandung, Bandung, Indonesia

Article history

Received

27 May 2022

Received in revised form

26 September 2022

Accepted

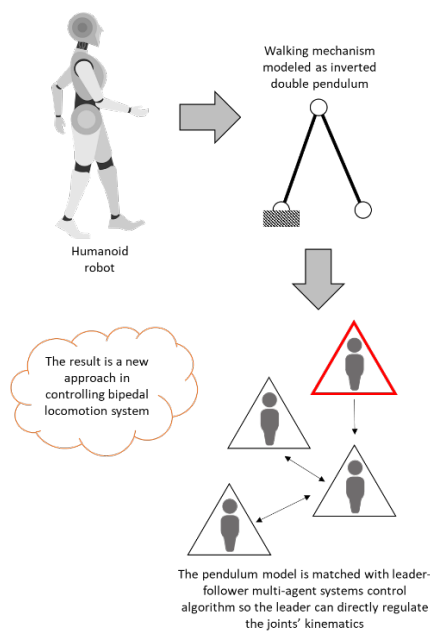
25 October 2022

Published online

28 February 2023

\*Corresponding author  
ipn@ftmd.itb.ac.id

## Graphical abstract



## Abstract

Robot that uses bipedal locomotion such as humanoid robot has a unique appeal in which the robot can perform many duties/works that cannot be done by wheeled robots due to spatial and environmental constraints. Related literature were about biped robots and robot arm that uses the concept of central pattern generator (CPG). Biped robots that use CPG (technically a neural oscillators) do not need any mathematical model of the robot itself. The controller "exploits" the dynamics of the robot to achieve an efficient way to drive the robot's joints. The driving frequency from this type of controller is thus heavily influenced by the dynamics of the robot it controls. One disadvantage of this method is that we cannot adjust the walking/movement parameter easily. Inspired by the idea of central pattern generator where one central "brain" controls the movement of the joints of the robot and the fact that the system uses neural oscillators reach some kind of "consensus", we are interested to study the feasibility of the implementation of leader – follower formation control based on consensus algorithm to bipedal locomotion system. The method studied in this report is to force the dynamic model of the double pendulum to match the kinematic model of the double integrator agent that uses consensus algorithm in forming formation. The walking/movement parameters of the robot using the proposed method are defined by one central "brain", and then the joints are working in consensus way to achieve the target joints' trajectories specified by the "brain". The study also concludes the notion of stability of the system driven by this controller which strongly related to the consensus ability in the context of Multi – Agent System.

**Keywords:** bipedal locomotion, multi-agent, leader-follower, consensus, inverted double-pendulum

© 2023 Penerbit UTM Press. All rights reserved

## 1.0 INTRODUCTION

To make humanoid robots look and behave as similar as possible to human, the development of bipedal locomotion or biped locomotion control on them is essential. Even so, the development of biped locomotion control for humanoid robots is still one of the most challenging research fields in robotics. As human uses ankle, hip, and stepping strategy in response to progressively increasing disturbance due to different environments, developing a controller which allow the

humanoid robots to have the same walking behavior as a human can increase their performance reliability [1].

To simulate biped locomotion on an uneven road, Santos et al. propose a controller based on a biomimetic CPG model [2]. They couple the used model to the body's biomechanical simulation and its interaction to its environment. The proposed controller is proven to allow the model to dynamically adapt in walking on roads with different slopes. Similarly, Auddy et al. in [3] also use CPG-based model to build their biped locomotion control. They introduce a neural network-based high-level CPG-based model controller to produce a stable walking humanoid

robot controller with less errors. The controller uses 2-D control signal and do not need explicit control on each joint.

Another study on biped locomotion control using CPG-based model has been done by [4]. They make a generic neural locomotion control for humanoid robots by combining CPG and radial basis function (RBF) network. The study demonstrates how CPG-RBF network is applied on a locomotion generation for the humanoid robots with different morphologies, then analyze it. It also shows how the choice of the encoding affects the morphology of the humanoid robots. The study also claims that the learned locomotion policy is applicable for the real-world robot and the possibility of integrating sensory feedback into the CPG-RBF network.

Besides the CPG-based model, a double pendulum can also be used as the model for the biped locomotion control development. A double pendulum is a pendulum where one pendulum is attached at the end of another pendulum. The double pendulum system has a very captivating non-linear behavior, which make it very suitable as walking humanoid robots also has this behavior [5]. The work [6], for example, propose the concept of Variable Double Inverted Pendulum (VDIP) for the static humanoid robot postures and Variable Double Inverted Pendulum on Cart (VDIPC) for the dynamic cases [6]. The study takes into human postures, both during the static and dynamic motion, to compare the human and the double pendulum behaviors. For the VDIPC, the study builds the pendulum state equations, which are formulated in the form suitable for model predictive control (MPC). Then, the preview control approach is applied. The study shows that VDIPC concept enables the design of the humanoid robot motion trajectories in accordance with the main joint masses.

In [7], Bahramian et al. proposes a double pendulum as a model for human walking control on a treadmill and same pace fluctuations. The study shows how a double pendulum can be used as a model for humanoid robot control development by considering two main steps in walking, single (when only one foot stepping on the ground) and double (when both feet stepping on the ground) support. In [8], Orhanli et al. also use the double pendulum as their model to analyze gait dynamics. The study uses Lagrangian Dynamics to derive the nonlinear equation of the gait. These studies show how the double pendulum model can simplify the mathematical computation of humanoid robot motion. However, for more complex situation, they are not sufficient compared to the derivation using VDIPC concept. Using this method, the walking parameters cannot be easily controlled. Even so, CPG model allow us to analyze without modeling the entire system. This advantage has motivated us to study the feasibility of the implementation of the leader-follower formation control based on the consensus algorithm to bipedal locomotion system.

The formation control using leader-follower based structure, which based on consensus control algorithm, allows us to control several agents into formation and perform formation tracking [9], [10]. In this work, we investigate the use of consensus-based formation control algorithm to the inverted double pendulum model for biped locomotion purpose. To the best of the authors' knowledge, no study has implemented the leader-follower formation control based on consensus algorithm to the inverted double pendulum model. First, we derive the double pendulum model. Then, the required torque at each joint is computed such that the closed-loop model follows the leader-follower formation control model.

Another method of leader-follower algorithm can be found in [11], which uses complex-laplacian approach. The limitation of the approach proposed by [11] is that it can only be applied to single integrator and double integrator dynamics. Meanwhile, the method applied in this work can be applied for higher order system.

## 2.0 METHODOLOGY

In studying the feasibility of implementation of leader – follower formation control based on consensus algorithm to bipedal locomotion, we first derive the mathematical model of double pendulum that represent the support leg and swing leg of a biped system. The problem is modeled only in sagittal – plane, also there are only two joints in the model (hip joint and ankle joint of the support leg). The upper body of the biped system were not considered in this work. We then derive the necessary and sufficient conditions for the modeled system to achieve consensus, hence stability, in view of its nonlinearity.

The torque at each joint is computed using state feedback control algorithm such that the state space equation of the linearized version follows the leader – follower structure based on consensus algorithm. Simulated problem is the model made to follow a step – like input mimicking how biped start to walk and to end a walking routine, and to follow a sinusoidal – like input mimicking dynamic walking of biped system where all joints are moving with certain frequencies and amplitude. The underlying graph in the communication network between the joints is assumed to be undirected and invariant (fixed) at each time step.

To realize the bipedal locomotion control, we consider two models: (i) the formation control of double integrator model and (ii) the bipedal locomotion model based on double inverted pendulum. Model matching technique is used to match the first model with the latter one so that the leg movement of the bipedal model follows the position trajectory of the double integrator model. Basically, the formation is achieved by firstly having agents in the double integrator model to reach consensus, then a bias is added so that they reach the formation. The advantage of using this method for bipedal locomotion is that each bipedal joint has their own controller, and the controller type is distributed. The central brain of the bipedal system need only to decide the leg movement, then the controller works independently. This is different from the centralized type of controller where the central controller computes the torque needed for all joint in the bipedal system. The advantage of distributed system we propose in this system is the scalability. The complexity of the controller remains the same no matter how many joints are used in the system.

In this section, we first discuss the results from multi-agent systems literature including graph theory, single integrator, and double integrator systems formation control. These results are needed to establish the foundation in deriving the bipedal locomotion control. Finally, we discuss the modeling of inverted double pendulum and the control law for the inverted double pendulum based on the leader-follower formation control.

## 2.1 Graph Notations and Existing Results in Cooperative Control of MASs

To apply the consensus algorithm into bipedal locomotion system, we need to consider communication or exchange of information between agents in the networked system. Agents in this context is the joint in the bipedal locomotion system. The communication network can be realized as a pure electronic communication via radio wave such that agent and its neighbors exchange information about its states.

To model the communication among agents in the networked system, we use graph (see [12]). A graph is made of vertices and edges connecting the vertices. Each agent is represented by one vertex in graph, and communication between agents is represented by the edges. In an undirected graph, when vertex  $i$  is connected by an edge to vertex  $j$ , it means that agent  $i$  is a neighbor to agent  $j$ . The graph  $G(V, E)$  or simply graph  $G$  is defined by a set of  $n$  vertices ( $V$ ) and a set of edges ( $E$ ). We say that agent  $i$  is a neighbor to agent  $j$  if  $(j, i) \in E$  for all  $i, j \in V$ .

To analyze the networked system algebraically, communication among agents is defined by using *Adjacency* matrix  $A = [a_{ij}] \in \mathbb{R}^{n \times n}$  defined by

$$\begin{aligned} a_{ij} &= 1 & (j, i) \in E \\ a_{ij} &= 0 & \text{otherwise} \end{aligned} \quad (1)$$

Also, we define the *Degree* matrix,  $D$ :

$$D = \text{diag}[d_1, d_2, \dots, d_n] \quad (2)$$

where  $d_i$  is the number of neighbors of agent  $i$ . And lastly, we define the Laplacian matrix,  $L$ :

$$L = D - A \quad (3)$$

For a simple graph which is discussed in this paper,  $a_{ii} = 0$ . For discussion on the property of Laplacian matrix, see [12], [13].

To review the leader-follower network in consensus algorithm, we first review consensus algorithm for single integrator agents given by:

$$\dot{x}_i = u_i; i = 1, 2, \dots, n \quad (4)$$

where  $x_i$  is the position of agent  $i$  and  $u_i$  is the control input of agent  $i$ . The control law based on consensus algorithm for system in (4) is given by [9]:

$$u_i = - \sum_{j=1}^n a_{ij}(x_i - x_j); i = 1, 2, \dots, n \quad (5)$$

Where  $a_{ij}$  is the  $i, j$  entry of the *Adjacency* matrix. The consensus-ability of system (4) by using control input (5) is discussed in [9]. Consensus is reached if as  $t \rightarrow \infty$ ,  $|x_i - x_j| \rightarrow 0$ .

In forming a formation (formation producing problem), the formation is said to be reached if as  $t \rightarrow \infty$ ,  $|x_i - x_j| \rightarrow |\delta_i - \delta_j|$ . Where  $\delta_i$  for all  $i$  is a variable that defines the target formation. To form a formation using consensus algorithm, the following control input is used:

$$u_i = - \sum_{j=1}^n a_{ij}[(x_i - x_j) - (\delta_i - \delta_j)] \quad (6)$$

for all  $i = 1, 2, \dots, n$

See [9], [12] for the discussion of formation control of single integrator agents.

To see how leader-follower network can be used in consensus or formation control, we can write the *Laplacian* matrix in general as follow:

$$L = \begin{bmatrix} d_1 & -a_{12} & \dots & -a_{1n} & -a_{1n} \\ -a_{21} & \ddots & \dots & \dots & -a_{2n} \\ \vdots & \vdots & \ddots & \dots & \vdots \\ -a_{n-1,1} & \vdots & \dots & d_{n-1} & -a_{n-1,n} \\ -a_{n1} & -a_{n2} & \dots & -a_{n,n-1} & d_n \end{bmatrix} \quad (7)$$

Without loss of generality, let the last agent (agent  $n$ ) to be the leader and the leader is assumed to take any arbitrary input, while the other agents called the follower assume the input described by equation (5). Therefore, we write the following as the leader – follower consensus algorithm:

$$\begin{aligned} u_i &= - \sum_{j=1}^n a_{ij}(x_i - x_j); i = 1, 2, \dots, n-1 \\ u_n &= u \end{aligned} \quad (8)$$

We can therefore write the *Laplacian* in this manner:

$$L = \begin{bmatrix} F & r \\ r^T & d_n \end{bmatrix} \quad (9)$$

Where  $F$  is obtained by deleting the last column and the last row of the Laplacian, and  $r$  is a  $n-1 \times 1$  vector, is the last column of the *Laplacian* without  $d_n$ . The equation of motion of the MAS can be written as the following:

$$\begin{bmatrix} \dot{x}_1(t) \\ \vdots \\ \dot{x}_{n-1}(t) \end{bmatrix} = -[F] \begin{bmatrix} x_1 \\ \vdots \\ x_{n-1} \end{bmatrix} - rx_n \quad (10)$$

While  $-L$  is Lyapunov stable with one zero eigenvalue,  $-F$  is stable [14]. Equation (10) then describe the leader – follower structure using consensus algorithm.

Let  $x = [x_1, x_2, \dots, x_{n-1}]^T$ ,  $z = x_n$ , and  $\delta = [\delta_1, \delta_2, \dots, \delta_{n-1}]^T$ . To form a formation, the same principle can be applied to equation (16) as we found on equation (10). We can thus write formation control dynamics based on equation (10) as follows:

$$\dot{x}(t) = -Fx(t) + F\delta(t) - rz(t) \quad (11)$$

If the input  $z(t) = 0$ , the formation of is solely defined by  $\delta(t)$ . The leader in the setting of equation (11) is also called as a virtual leader, because  $z(t)$  can be regarded as a virtual input to the agent connected to the leader node; and agent  $n$  is not necessarily a physical agent. For a constant  $\delta$ , the asymptotic value of the agents' states is the following:

$$\lim_{t \rightarrow \infty} x(t) = \delta \quad (12)$$

While for  $\delta$  as a function of time, the solution of the states become:

$$x(t) = \bar{M}(e^{-\Lambda t}) \left( \int_0^t \begin{bmatrix} e^{\lambda_1 \tau} \bar{m}_1^T \\ e^{\lambda_2 \tau} \bar{m}_2^T \\ \vdots \\ e^{\lambda_{n-1} \tau} \bar{m}_{n-1}^T \end{bmatrix} \begin{bmatrix} d_1 \delta_1(\tau) - \sum_{j=2}^{n-1} a_{1j} \delta_j(\tau) \\ d_2 \delta_2(\tau) - \sum_{j=2}^{n-1} a_{2j} \delta_j(\tau) \\ \vdots \\ d_{n-1} \delta_{n-1}(\tau) - \sum_{j=1}^{n-2} a_{nj} \delta_j(\tau) \end{bmatrix} d\tau \right) \quad (13)$$

Where  $\bar{M}$  is a matrix containing eigenvector of matrix  $F$ ,  $\bar{\Lambda}$  is a diagonal matrix with eigenvalues of  $F$  as its entries, and  $\bar{m}_i$  for  $i = 1, 2, \dots, n - 1$  is the column entry of matrix  $\bar{M}$ .

When agents' dynamics is double integrator, we consider the following model:

$$\begin{aligned} \dot{x}_i &= v_i \\ \dot{v}_i &= u_i \end{aligned} \quad (14)$$

for  $i = 1, 2, \dots, n$ , where  $x_i$  is the position of agent  $i$ ,  $v_i$  is the velocity of agent  $i$  and  $u_i$  is the control input of agent  $i$ . To form the formation, based on [9], the control law for each agent is defined as:

$$u_i = - \sum_{j=1}^n a_{ij} [(x_i - x_j) + \alpha(v_i - v_j) - (\delta_i - \delta_j) - \alpha(\gamma_i - \gamma_j)] \quad (15)$$

where  $\alpha$  is a nonzero constant. Let  $x = [x_1, x_2, \dots, x_n]^T$  and  $v = [v_1, v_2, \dots, v_n]^T$ , the whole agents' dynamics are:

$$\begin{bmatrix} \dot{x}(t) \\ \dot{v}(t) \end{bmatrix} = \begin{bmatrix} 0 & I \\ -L & -\alpha L \end{bmatrix} \begin{bmatrix} x(t) \\ v(t) \end{bmatrix} + \begin{bmatrix} 0 & I \\ L & \alpha L \end{bmatrix} \begin{bmatrix} \delta(t) \\ \gamma(t) \end{bmatrix} \quad (16)$$

Where  $\delta$  and  $\gamma$  are the target formation for state  $x$  and  $v$  respectively.

Analogue to equation (11), we can set one agent to be the leader and obtain the following state space equation:

$$\begin{bmatrix} \dot{x}(t) \\ \dot{v}(t) \end{bmatrix} = \begin{bmatrix} 0 & I \\ -F & -\alpha F \end{bmatrix} \begin{bmatrix} x(t) \\ v(t) \end{bmatrix} + \begin{bmatrix} 0 & 0 \\ F & \alpha F \end{bmatrix} \begin{bmatrix} \delta(t) \\ \gamma(t) \end{bmatrix} + \begin{bmatrix} 0 & 0 \\ -r & -\alpha r \end{bmatrix} \begin{bmatrix} z \\ \dot{z} \end{bmatrix} \quad (17)$$

Where  $z$  and  $\dot{z}$  are the leader's state and its derivative respectively. We now assume that the number of the follower is  $n$ , and thus  $F$  is a matrix of  $n \times n$ . By setting the leader's state and its derivative to be zero, we are interested to derive the solution of equation (17). We rewrite equation (17) as follows:

$$\begin{aligned} \dot{y}(t) &= Hy(t) + Q\eta(t) \\ H &= \begin{bmatrix} 0 & I \\ -F & -\alpha F \end{bmatrix}; y(t) = \begin{bmatrix} x(t) \\ v(t) \end{bmatrix} \\ Q &= \begin{bmatrix} 0 & 0 \\ F & \alpha F \end{bmatrix}; \eta(t) = \begin{bmatrix} \delta(t) \\ \gamma(t) \end{bmatrix} \end{aligned} \quad (18)$$

The solution of equation (18) is then:

$$y(t) = e^{Ht}y(0) + \int_0^t e^{H(t-\tau)} Q\eta(\tau) d\tau \quad (19)$$

Knowing that the eigenvalues of  $H$  are all negative when the underlying graph of the Laplacian is connected [9], the first term of the RHS equation (19) will be reduced to zero after some time. And thus, after the transient response part is gone, equation (19) reduces to:

$$y(t) = e^{Ht}N \int_0^t \begin{bmatrix} \Phi_2(\tau)F & \alpha\Phi_2(\tau)F \\ \Phi_4(\tau)F & \alpha\Phi_4(\tau)F \end{bmatrix} \eta(\tau) d\tau \quad (20)$$

Where for constant  $\eta$ , the asymptotic value of  $y$  is:

$$\lim_{t \rightarrow \infty} y(t) = -H^{-1}Q\eta = \begin{bmatrix} \delta + \alpha\gamma \\ 0 \end{bmatrix} \quad (21)$$

In addition, if  $\gamma = 0$ , the asymptotic value of  $y$  is:

$$\lim_{t \rightarrow \infty} y(t) = \lim_{t \rightarrow \infty} \begin{bmatrix} x(t) \\ v(t) \end{bmatrix} = \begin{bmatrix} \delta \\ 0 \end{bmatrix} \quad (22)$$

For the case of double integrator agent, agents are said to reach formation if as  $t \rightarrow \infty$ ,  $|x_i - x_j| \rightarrow |\delta_i - \delta_j|$  and  $|v_i - v_j| \rightarrow 0$ . Equation (22) is valid if and only if the underlying graph of the system's matrix is connected.

The discussion in this section considers kinematic model of the agent, be it single integrator or double integrator. In the next section, we will use the same method as the double integrator (kinematic model) consensus to the dynamic model of the joints (agent) of the double pendulum (which is also a double integrator type) to form a formation.

### 2.2 Mathematical Modeling of Inverted Double Pendulum

To approximate the dynamics of biped system, we use the inverted double pendulum model, inspired by the Linear Inverted Pendulum Model discussed in [15]. The upper body is not fully modeled in this paper. Also, the joints modeled are only the hip joint and the ankle joint of the support leg. Figure 2 shows the schematic of the double pendulum used in this paper.

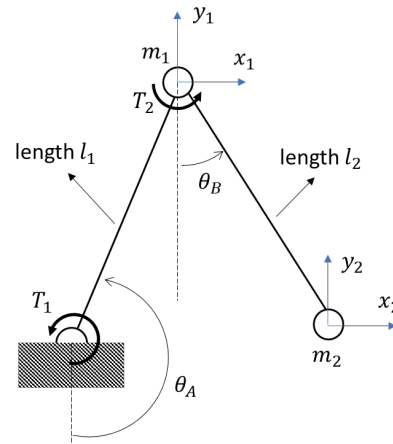


Figure 1. Schematic of inverted double pendulum

In the inverted double pendulum model of Figure 1, link 1 with length of  $l_1$  is the support leg, while the link 2 with length of  $l_2$  is the swing leg.  $\theta_A$  is the angle between the support leg and the vertical line reference. In this paper, the default value of  $\theta_A$  is  $\pi$  (position of standing upright).  $\theta_B$  is the angle between the swing leg and the vertical line reference, and its default value is 0.  $T_1$  and  $T_2$  are the torque at the ankle joint and hip joint, respectively. The mass of the upper body is modeled as a point at the hip joint ( $m_1$ ), while the mass of the swing leg is modeled as a point at the end of the link 2 ( $m_2$ ). Meanwhile,  $(x_1, y_1)$  and  $(x_2, y_2)$  are the Cartesian coordinate of each point mass w.r.t. point O, respectively. The Cartesian coordinate for each mass are as follows:

$$\begin{aligned} x_1 &= l_1 \sin \theta_A \\ y_1 &= -l_1 \cos \theta_A \\ x_2 &= x_1 + l_2 \sin \theta_B = l_1 \sin \theta_A + l_2 \sin \theta_B \\ y_2 &= y_1 - l_2 \cos \theta_B = -l_1 \cos \theta_A - l_2 \cos \theta_B \end{aligned} \quad (23)$$

We use the Lagrangian approach to derive the equation of motion of the double pendulum:

$$\frac{d}{dt} \left( \frac{\partial L}{\partial \dot{\theta}_i} \right) - \frac{\partial L}{\partial \theta_i} = T_i \quad (24)$$

Where:

$$L = E_k - E_p \quad (25)$$

$L$  in equation (25) is not to be confused with the *Laplacian*.  $E_k$  is the kinetic energy and  $E_p$  is the potential energy. The full derivation of the equation of motion is given in Appendix. Let  $\bar{T}_2 = T_1 - T_2$ , following is the worked nonlinear state space equation of the double pendulum based on the model of Figure 2 (see Appendix A for the derivation):

$$\theta_A = \theta_1; \theta_B = \theta_3$$

$$\dot{\theta}_1 = \theta_2$$

$$\dot{\theta}_2 = p \begin{bmatrix} \frac{T_1}{l_1^2} - \frac{T_2 \cos(\theta_1 - \theta_3)}{l_1 l_2} & \\ -\theta_2^2 m_2 \sin(\theta_1 - \theta_3) \cos(\theta_1 - \theta_3) - \frac{\theta_4^2 m_2 l_2 \sin(\theta_1 - \theta_3)}{l_1} & \\ + \frac{m_2 g \cos(\theta_1 - \theta_3) \sin \theta_3}{l_1} - \frac{(m_1 + m_2) g \sin \theta_1}{l_1} & \end{bmatrix} \quad (26)$$

$$\dot{\theta}_4 = (m_1 + m_2) p \begin{bmatrix} \frac{\bar{T}_2}{m_2 l_2^2} - \frac{T_1 \cos(\theta_1 - \theta_3)}{l_1 l_2 (m_1 + m_2)} & \\ + \frac{\theta_2^2 \sin(\theta_1 - \theta_3) \cos(\theta_1 - \theta_3)}{(m_1 + m_2)} + \frac{g \sin \theta_1 \cos(\theta_1 - \theta_3)}{l_2} & \\ + \frac{\theta_4^2 l_1 \sin(\theta_1 - \theta_3)}{l_2} - \frac{g \sin \theta_3}{l_2} & \end{bmatrix}$$

$$p = \frac{1}{m_1 + m_2 - m_2 \cos(\theta_1 - \theta_3)^2}$$

### 2.3 Computation of the Control Law of the Inverted Double Pendulum

To define the control law for the inverted double pendulum model, we first linearize equation (34) as follows:

$$\begin{aligned} \delta \dot{\theta}_1 &= \delta \theta_2 \\ \delta \dot{\theta}_2 &= a_1 \delta \theta_1 + a_2 \delta \theta_2 + a_3 \delta \theta_3 + a_4 \delta \theta_4 + a_5 \delta T_1 + a_6 \delta \bar{T}_2 \\ \delta \dot{\theta}_3 &= \delta \theta_4 \\ \delta \dot{\theta}_4 &= b_1 \delta \theta_1 + b_2 \delta \theta_2 + b_3 \delta \theta_3 + b_4 \delta \theta_4 + b_5 \delta T_1 + b_6 \delta \bar{T}_2 \end{aligned} \quad (27)$$

where  $\delta(\cdot)$  defines the linearized states and inputs. Equation (35) can be written in matrix form as follows:

$$\begin{bmatrix} \delta \dot{\theta}_1 \\ \delta \dot{\theta}_2 \\ \delta \dot{\theta}_3 \\ \delta \dot{\theta}_4 \end{bmatrix} = \begin{bmatrix} 0 & 0 & 1 & 0 \\ 0 & 0 & 0 & 1 \\ a_1 & a_2 & a_3 & a_4 \\ b_1 & b_2 & b_3 & b_4 \end{bmatrix} \begin{bmatrix} \delta \theta_1 \\ \delta \theta_2 \\ \delta \theta_3 \\ \delta \theta_4 \end{bmatrix} + \begin{bmatrix} 0 & 0 \\ 0 & 0 \\ a_5 & a_6 \\ b_5 & b_6 \end{bmatrix} \begin{bmatrix} \delta T_1 \\ \delta \bar{T}_2 \end{bmatrix} \quad (28)$$

The coefficients of  $a_1$  to  $a_6$  and  $b_1$  to  $b_6$  are given in the Appendix. The torque  $\delta T_1$  and  $\delta \bar{T}_2$  are computed such that equation (28) perfectly match the format of equation (18) which is the leader – follower formation control using consensus algorithm. We then define the torques as follows:

$$\begin{aligned} \begin{bmatrix} \delta T_1 \\ \delta \bar{T}_2 \end{bmatrix} &= -K \delta \theta + W \delta \theta^* \\ &= - \begin{bmatrix} k_1 & k_2 & k_3 & k_4 \\ k_5 & k_6 & k_7 & k_8 \end{bmatrix} \begin{bmatrix} \delta \theta_1 \\ \delta \theta_2 \\ \delta \theta_3 \\ \delta \theta_4 \end{bmatrix} + \begin{bmatrix} w_1 & w_2 & w_3 & w_4 \\ w_5 & w_6 & w_7 & w_8 \end{bmatrix} \begin{bmatrix} \delta \theta_1^* \\ \delta \theta_2^* \\ \delta \theta_3^* \\ \delta \theta_4^* \end{bmatrix} \end{aligned} \quad (29)$$

Where  $\delta \theta_i^*$  defines the desired  $\delta \theta_i$ . By substituting equation (37) to equation (36) we obtain the following linear state space equation:

$$\begin{bmatrix} \delta \dot{\theta}_1 \\ \delta \dot{\theta}_2 \\ \delta \dot{\theta}_3 \\ \delta \dot{\theta}_4 \end{bmatrix} = \begin{bmatrix} 0 & 0 & 1 & 0 \\ a_1 - (a_2 k_1 + a_6 k_5) & a_3 - (a_2 k_2 + a_6 k_6) & a_2 - (a_2 k_3 + a_6 k_7) & a_4 - (a_2 k_4 + a_6 k_8) \\ b_1 - (b_2 k_1 + b_6 k_5) & b_3 - (b_2 k_2 + b_6 k_6) & b_2 - (b_2 k_3 + b_6 k_7) & b_4 - (b_2 k_4 + b_6 k_8) \\ 0 & 0 & 0 & 0 \\ 0 & 0 & 0 & 0 \\ (a_5 w_1 + a_6 w_5) & (a_5 w_2 + a_6 w_6) & (a_5 w_3 + a_6 w_7) & (a_5 w_4 + a_6 w_8) \\ (b_5 w_1 + b_6 w_5) & (b_5 w_2 + b_6 w_6) & (b_5 w_3 + b_6 w_7) & (b_5 w_4 + b_6 w_8) \end{bmatrix} \begin{bmatrix} \delta \theta_1 \\ \delta \theta_2 \\ \delta \theta_3 \\ \delta \theta_4 \end{bmatrix} + \begin{bmatrix} \delta \theta_1^* \\ \delta \theta_2^* \\ \delta \theta_3^* \\ \delta \theta_4^* \end{bmatrix} \quad (30)$$

In view of equation (30), the angular position of link 1 (support leg) and link 2 (swing leg) can be controlled through  $\delta \theta_1^*, \delta \theta_3^*, \delta \theta_2^*, \theta_4^*$ . In this report, we assume that the target formation  $(\delta \theta_1^*, \delta \theta_3^*, \delta \theta_2^*, \theta_4^*)$  can be influenced directly by the central “brain” of the system, so that these values are not determined by each joint (each agent) themselves.

We assume that the ankle joint and the hip joint are the follower agent in a 3 multi-agent configuration, where the third agent is a virtual leader. The purpose of this setting is such that the values  $\theta_A$  and  $\theta_B$  and their derivatives can be regulated using equation (26). Therefore, the only possible graph that can be constructed are the path graph and complete graph:

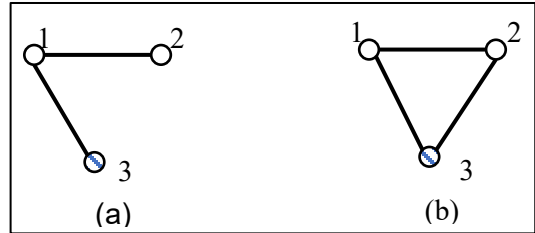


Figure 2. Path graph (a) and complete graph (b) for 3 agents’ system (agent 3 is the virtual leader)

Following are the Laplacian and the matrix  $F$  for both path graph and complete graph of Figure 2:

$$\begin{aligned} L_{path} &= \begin{bmatrix} 2 & -1 & -1 \\ -1 & 1 & 0 \\ -1 & 0 & 1 \end{bmatrix}; F_{path} = \begin{bmatrix} 2 & -1 \\ -1 & 1 \end{bmatrix} \\ L_{complete} &= \begin{bmatrix} 2 & -1 & -1 \\ -1 & 2 & -1 \\ -1 & -1 & 2 \end{bmatrix}; F_{complete} = \begin{bmatrix} 2 & -1 \\ -1 & 2 \end{bmatrix} \end{aligned} \quad (31)$$

To compute the controller for arbitrary network (as long as it is connected), we parameterized the matrix  $F$  as follow:

$$F = \begin{bmatrix} f_{11} & f_{12} \\ f_{21} & f_{22} \end{bmatrix} \quad (32)$$

We can then get the following relationships to compute the matrix  $K$  and  $W$  in equation (37):

$$\begin{bmatrix} -a_5 & -a_6 \\ -b_5 & -b_6 \end{bmatrix} \begin{bmatrix} k_1 \\ k_5 \end{bmatrix} = \begin{bmatrix} -f_{11} - a_1 \\ -f_{21} - b_1 \end{bmatrix} \quad (33.a)$$

$$\rightarrow \begin{bmatrix} k_1 \\ k_5 \end{bmatrix} = \begin{bmatrix} -a_5 & -a_6 \\ -b_5 & -b_6 \end{bmatrix}^{-1} \begin{bmatrix} -f_{11} - a_1 \\ -f_{21} - b_1 \end{bmatrix}$$

$$\begin{bmatrix} -a_5 & -a_6 \\ -b_5 & -b_6 \end{bmatrix} \begin{bmatrix} k_2 \\ k_6 \end{bmatrix} = \begin{bmatrix} -f_{12} - a_3 \\ -f_{22} - b_3 \end{bmatrix} \quad (33.b)$$

$$\rightarrow \begin{bmatrix} k_2 \\ k_6 \end{bmatrix} = \begin{bmatrix} -a_5 & -a_6 \\ -b_5 & -b_6 \end{bmatrix}^{-1} \begin{bmatrix} -f_{12} - a_3 \\ -f_{22} - b_3 \end{bmatrix}$$

$$\begin{bmatrix} -a_5 & -a_6 \\ -b_5 & -b_6 \end{bmatrix} \begin{bmatrix} k_3 \\ k_7 \end{bmatrix} = \begin{bmatrix} -\alpha f_{11} - a_2 \\ -\alpha f_{21} - b_2 \end{bmatrix} \quad (33.c)$$

$$\rightarrow \begin{bmatrix} k_3 \\ k_7 \end{bmatrix} = \begin{bmatrix} -a_5 & -a_6 \\ -b_5 & -b_6 \end{bmatrix}^{-1} \begin{bmatrix} -\alpha f_{11} - a_2 \\ -\alpha f_{21} - b_2 \end{bmatrix}$$

$$\begin{bmatrix} -a_5 & -a_6 \\ -b_5 & -b_6 \end{bmatrix} \begin{bmatrix} k_4 \\ k_8 \end{bmatrix} = \begin{bmatrix} -\alpha f_{12} - a_4 \\ -\alpha f_{22} - b_4 \end{bmatrix} \quad (33.d)$$

$$\rightarrow \begin{bmatrix} k_4 \\ k_8 \end{bmatrix} = \begin{bmatrix} -a_5 & -a_6 \\ -b_5 & -b_6 \end{bmatrix}^{-1} \begin{bmatrix} -\alpha f_{12} - a_4 \\ -\alpha f_{22} - b_4 \end{bmatrix}$$

$$\begin{bmatrix} a_5 & a_6 \\ b_5 & b_6 \end{bmatrix} \begin{bmatrix} w_1 \\ w_5 \end{bmatrix} = \begin{bmatrix} f_{11} \\ f_{21} \end{bmatrix} \quad (34.a)$$

$$\rightarrow \begin{bmatrix} w_1 \\ w_5 \end{bmatrix} = \begin{bmatrix} a_5 & a_6 \\ b_5 & b_6 \end{bmatrix}^{-1} \begin{bmatrix} f_{11} \\ f_{21} \end{bmatrix}$$

$$\begin{bmatrix} a_5 & a_6 \\ b_5 & b_6 \end{bmatrix} \begin{bmatrix} w_2 \\ w_6 \end{bmatrix} = \begin{bmatrix} f_{12} \\ f_{22} \end{bmatrix} \quad (34.b)$$

$$\rightarrow \begin{bmatrix} w_2 \\ w_6 \end{bmatrix} = \begin{bmatrix} a_5 & a_6 \\ b_5 & b_6 \end{bmatrix}^{-1} \begin{bmatrix} f_{12} \\ f_{22} \end{bmatrix}$$

$$\begin{bmatrix} a_5 & a_6 \\ b_5 & b_6 \end{bmatrix} \begin{bmatrix} w_3 \\ w_7 \end{bmatrix} = \begin{bmatrix} \alpha f_{11} \\ \alpha f_{21} \end{bmatrix} \quad (34.c)$$

$$\rightarrow \begin{bmatrix} w_3 \\ w_7 \end{bmatrix} = \begin{bmatrix} a_5 & a_6 \\ b_5 & b_6 \end{bmatrix}^{-1} \begin{bmatrix} \alpha f_{11} \\ \alpha f_{21} \end{bmatrix}$$

$$\begin{bmatrix} a_5 & a_6 \\ b_5 & b_6 \end{bmatrix} \begin{bmatrix} w_4 \\ w_8 \end{bmatrix} = \begin{bmatrix} \alpha f_{12} \\ \alpha f_{22} \end{bmatrix} \quad (34.d)$$

We note that in equations (33) and (34),  $\begin{bmatrix} a_5 & a_6 \\ b_5 & b_6 \end{bmatrix}$  must be nonsingular. To check this, we can observe this matrix as the following (see Appendix for the value of the coefficient):

$$\begin{bmatrix} a_5 & a_6 \\ b_5 & b_6 \end{bmatrix} = \frac{1}{p} \begin{bmatrix} \frac{1}{l_1^2} & \frac{-\cos(\theta_1 - \theta_3)}{l_1 l_2} \\ -\frac{\cos(\theta_1 - \theta_3)}{l_1 l_2} & \frac{(m_1 + m_2)}{l_2^2 m_2} \end{bmatrix} \quad (35)$$

From equation (35), we can see that the diagonal of  $\begin{bmatrix} a_5 & a_6 \\ b_5 & b_6 \end{bmatrix}$  is nonzero for any angular position of link 1 and link 2 ( $\theta_1$  and  $\theta_3$ ). Furthermore, this matrix will be singular if:

$$\frac{-\cos(\theta_1 - \theta_3)}{l_1 l_2} = \frac{(m_1 + m_2)}{-\cos(\theta_1 - \theta_3)} \Rightarrow \cos^2(\theta_1 - \theta_3) = \frac{(m_1 + m_2)}{m_2} \quad (36)$$

that is if the 2 columns are dependent. Equation (36) shows that this is not possible for any angular position of link 1 and link 2, because the LHS of equation (36) has maximum value of 1, and the RHS will always be greater than 1, that is  $m_1$  cannot be zero. This analysis also shows that the control law can be computed at any linearization point.

By taking the form of equation (18), the control law proposed in this paper results in stable closed-loop linearized model of the pendulum. This is due to matrix  $H$  in (18) is Hurwitz when the graph is connected.

## 3.0 RESULTS AND DISCUSSION

### 3.1 Simulation of the Linear Inverted Double Pendulum at Default Linearization Point

To simulate the linear inverted double pendulum model in MATLAB®, we linearize equation (26) about  $\theta_1 = \pi; \theta_3 = \theta_2 = \theta_4 = T_1 = \bar{T}_2 = 0$  (default linearization point). We assume that the network between agents (joints) are path network, and thus we parameterized matrix  $F$  as follows:

$$F = \begin{bmatrix} f_{11} & f_{12} \\ f_{21} & f_{22} \end{bmatrix} = \beta \begin{bmatrix} 2 & -1 \\ -1 & 1 \end{bmatrix}; \beta > 0 \quad (37)$$

The role of  $\beta$  is to scale up the eigenvalues of matrix  $F$ . What we will study in the simulation is the effect of  $\alpha$  and  $\beta$  to the transient and steady state response of the system due to step-like and sinusoidal-like target formation variable ( $\delta\theta_1^*, \delta\theta_3^*, \delta\theta_2^*, \theta_4^*$ ). Throughout the simulation, we set  $\delta\theta_2^* = \delta\theta_4^* = 0$ , which means the target angular velocity of the joints are zero. Table 1 shows the double pendulum model parameter used in the simulation.

Table 1. Parameter of the Double Pendulum in the Simulation

Parameter	Value
$l_1$	1 m
$l_2$	1 m
$m_1$	2 kg
$m_2$	2 kg

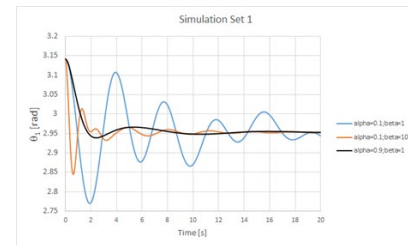
Following is the linearized state space equation about  $\theta_1 = \pi; \theta_3 = \theta_2 = \theta_4 = T_1 = \bar{T}_2 = 0$ :

$$\begin{bmatrix} \delta\dot{\theta}_1 \\ \delta\dot{\theta}_3 \\ \delta\dot{\theta}_2 \\ \delta\dot{\theta}_4 \end{bmatrix} = \begin{bmatrix} 0 & 0 & 1 & 0 \\ 0 & 0 & 0 & 1 \\ 19.62 & -9.81 & 0 & 0 \\ 19.62 & -19.62 & 0 & 0 \end{bmatrix} \begin{bmatrix} \delta\theta_1 \\ \delta\theta_3 \\ \delta\theta_2 \\ \delta\theta_4 \end{bmatrix} + \begin{bmatrix} 0 & 0 \\ 0 & 0 \\ 0.5 & 0.5 \\ 0.5 & 1 \end{bmatrix} \begin{bmatrix} \delta T_1 \\ \delta \bar{T}_2 \end{bmatrix} \quad (38)$$

With the torques computed using equations (29), (33), and (34), following are the states' response of the system:

#### 3.1.1. States' responses with initial condition of $\theta_1 = \pi; \theta_3 = \theta_2 = \theta_4 = 0$ and target formation $\delta\theta_1^* = 0.94\pi, \delta\theta_3^* = 0.06\pi$ ; step type target formation (simulation set 1)

From Figures 3 and 4, the steady state responses of the double pendulum follow equation (22).



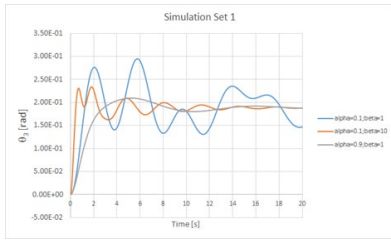


Figure 3. Angular position responses of link 1 and link 2

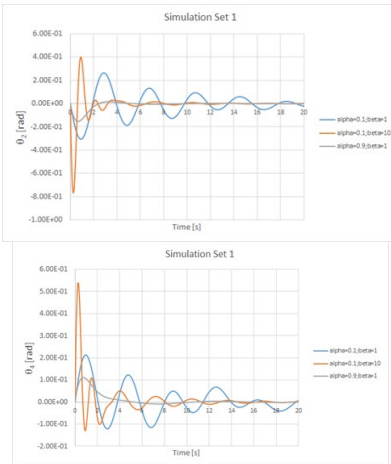


Figure 4 Angular velocity responses of link 1 and link 2

We can see that  $\beta$  directly affects the speed of the response because it affects the eigenvalues of the system’s matrix directly, also we can see that  $\alpha$  affects the damping ratio of the system. In view of bipedal locomotion system, it is desirable to have quick response with sufficient damping so that the system settles as fast as possible.

**3.1.2. States’ Responses With Initial Condition Of  $\theta_1 = \pi; \theta_3 = \theta_2 = \theta_4 = 0$  And Target Formation  $\delta\theta_1^* = \pi + 0.1\pi \sin(2\pi t), \delta\theta_3^* = 0.1\pi \sin(4\pi t)$  ; Sinusoidal Type Target Formation (Simulation Set 2)**

In this simulation, the target formation is a sinusoidal function. We deliberately set the frequency target for link 2 to be higher than the frequency target of link 1 to see how well the system can follow the sinusoidal type of target formation. Three kinds of setting of  $\alpha$  and  $\beta$  will be compared:

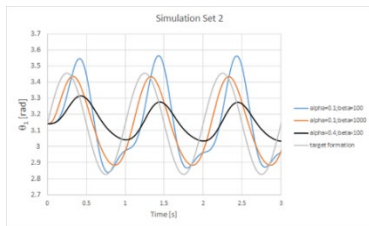


Figure 5. Angular position response of link 1 to sinusoidal input

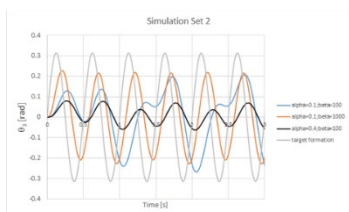


Figure 6. Angular position response of link 2 to sinusoidal input

From Figures 5 and 6, it can be observed that the settings of  $\alpha$  and  $\beta$  resulting in the system to follow the sinusoidal input quite well is high  $\beta$  and low  $\alpha$ .

**3.2 Simulation of the Nonlinear Model of Inverted Double Pendulum Model**

Simulation results at section 3.1 shows that the leader – follower formation control scheme based on consensus algorithm works well for constant type and sinusoidal type of target formations. However, the results at section 3.1 are valid only for the chosen linearization points ( $\theta_1 = \pi; \theta_3 = \theta_2 = \theta_4 = T_1 = T_2 = 0$ ), that is if the full nonlinear model operates around these points.

Suppose we want to use the proposed controller in section 2.3, which is a linear controller, for the full nonlinear model; since the full nonlinear model cannot be forced to operate with very small deviation from the linearization points, we need to have more than one linearization points to compute the proper controller. With different linearization points, the state space equation (30) will not hold anymore, and we cannot use the same matrices  $K$  and  $W$  that were computed based on equation (30) in the control law. We need to use the state of the full model at each time step as the linearization points and then update these feedback matrices ( $K$  and  $W$ ) accordingly. This way, we ensure that each time step, the linearized model of equation (18) match the format of the leader – follower formation control based on consensus algorithm (equation (18)). The nonlinear model is simulated using ODE45 routine in MATLAB®.

Following are the simulation results on the equation (34) using  $\alpha = 0.3$  and  $\beta = 200$

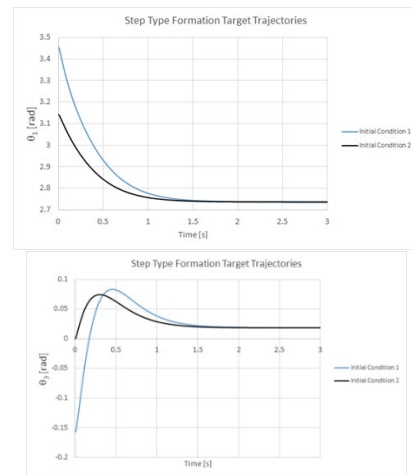
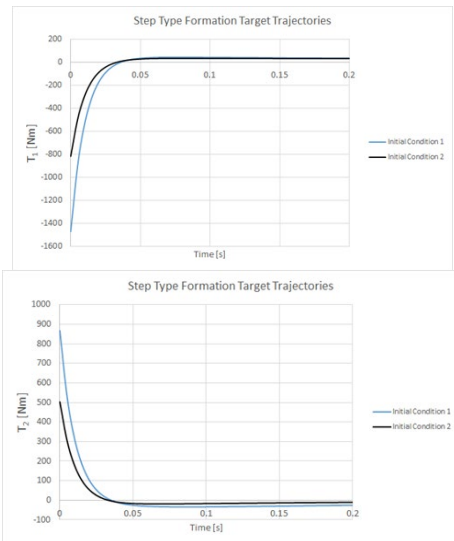


Figure 7. Angular position response of link 1 (left) and link 2 (right) for  $\delta\theta_1^* = 0.9\pi, \delta\theta_3^* = 0.05\pi$ . Initial condition 1: ( $\theta_1(0) = 1.1\pi; \theta_3(0) = -0.05; \theta_2(0) = -0.1; \theta_4(0) = -0.05$ ) . Initial condition 2: ( $\theta_1(0) = \pi; \theta_3(0) = 0; \theta_2(0) = 0; \theta_4(0) = 0$ ).



**Figure 8.** Torque at ankle joint ( $T_1$ ) and hip joint ( $T_2$ ) for step type input and response of Figure 7.

From the results of Figures 7 to 10, the system can follow the given trajectories quite well. The speed of the response is affected by both  $\alpha$  and  $\beta$  settings and also the choice of graph topology. It is known that the *Laplacian* of path graph topology has small eigenvalue compared to complete graph topology. Therefore, we can still tune the graph topology should we find the  $\alpha$  and  $\beta$  settings not suitable for a given purpose. Referring to [16], the average walking pace of human is 2.5 mph or 1.1 m/s, and thus average human can finish the step type movement from the simulation of Figure 8 in around 1 second. Meanwhile, the simulation of Figure 8 shows that the system reaches steady state in around 2 seconds. We believe that this response time is still acceptable for bipedal locomotion application.

We can also observe that the torques at joints are strongly affected by the sharpness of the target formation trajectories. If the trajectories are very sharp, like step input, the torque needed is very high. But for a ramp type input, represented by the sinusoidal trajectories, the torque needed is relatively small.

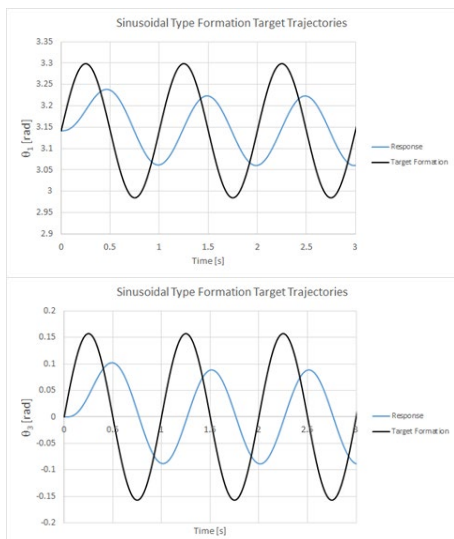


**Figure 9.** Angular position response of link 1 (left) and link 2 (right) for  $\delta\theta_1^* = \pi + 0.1\pi \sin(2\pi t)$ ,  $\delta\theta_3^* = 0.05\pi \sin(2\pi t)$ . Initial conditions:  $(\theta_1(0) = \pi; \theta_3(0) = 0; \theta_2(0) = 0; \theta_4(0) = 0)$

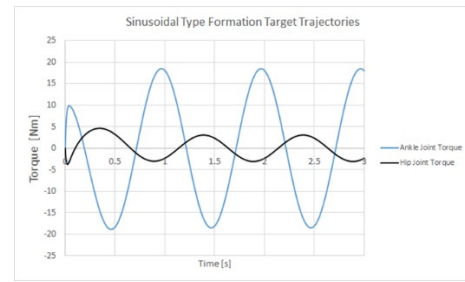


**Figure 10.** Torques at ankle joint and hip joint for sinusoidal type input

Simulation results of Figure 7 shows the approximation of the biped to start walking from upright position (initial condition 2), and to continue the walking routine (initial condition 1). To better illustrate the bipedal system movement, the screenshot of the animation from simulation of Figure 7 (initial condition 1) is shown in Figure 11.

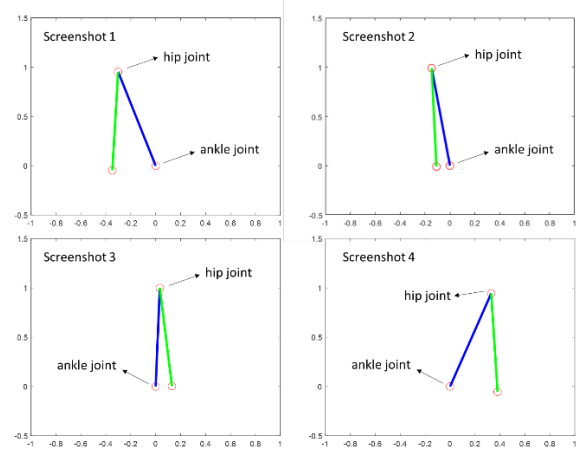


**Figure 11.** Screenshot of animation of bipedal system

### 3.3 Notion of Stability

Inspired by limit cycle and the input-output stability (see [17]), we define stability in the problem of the inverted double pendulum in this paper as the ability of the system to follow the target formation trajectories asymptotically. In other words, the error between the joints' responses and the target formation trajectories must be bounded. It means that the notion of stability proposed in this paper is the ability of the system to match the linearized version of the nonlinear model at each time step to the leader – follower formation control based on consensus algorithm structure (equation (18)). It also means that we must keep the linearized system to stay connected at each time step. When the linearized system is not connected (the graph is not connected), the asymptotic responses of the system will not follow the target formation (equations (21) and (22)), causing the responses of the system to drift away from the target formation. We can conclude that the stability of the system in this problem is the consensus – ability of the linearized system. The system in this problem is stable if and only if the linearized system can reach consensus at each time step.

The stability condition for the simulation result of Figure 7 is clear, since we use a constant (step type) target formation trajectory. To see stability condition from the result of Figure 9, Figure 12 shows the evolution of the error between the joints' responses and target formation trajectories. Figure 12 shows that the error between the joints' responses and target

formation trajectories are bounded. One possible reason where this method cannot keep the system to be stable is if the torques at joints are saturated.

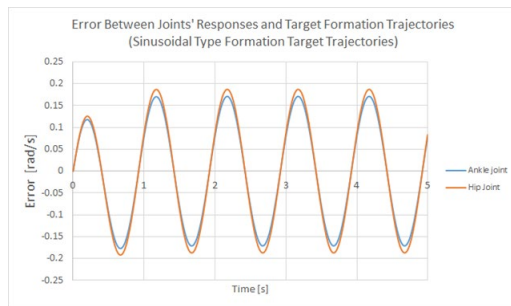


**Figure 12** Error between joints' responses and target formation trajectories of simulation results from Figure 9

#### 4.0 CONCLUSION

The leader – follower formation control based on consensus algorithm can be applied to the double pendulum system to control the trajectories of the joints of the double pendulum. The concept is to force the dynamic model of the double pendulum to match the kinematic model of double integrator in equation (18). We conclude that the system in this work is stable if and only if the linearized system can reach consensus at each time step (if and only if the underlying graph of the linearized system is connected).

It has been shown that the trajectories of the joints can be directly influenced by the settings of the target formation, not only the amplitude but also its frequency can also be influenced. This ability of the proposed system suits the needs of the bipedal locomotion system where we want to set the walking parameter easily. Some disadvantages of the proposed method include: (1) the stability of the system is very sensitive to the availability of the torques at joints to make the linearized system stays connected, hence torque saturation will directly lead to instability, (2) the control law in the proposed system is model dependent and the study on model imperfection effect to stability has not been done yet. The method studied in this report also depends on the states to compute the torques (state feedback). We need angular displacement as well as angular velocity sensors at each joint to make this method works. This could lead to expensive implementation of this method to real biped systems. Future work from this research includes the consideration of model uncertainties and disturbance to the system, which is a real-world problem in control system.

#### Acknowledgement

This research is supported by CRCS of Sampoerna University and Faculty of Mechanical and Aerospace Engineering of Institut Teknologi Bandung.

#### References

- [1] M. Shafiee-Ashtiani, A. Yousefi-Koma, and M. Shariat-Panahi, 2017. "Robust bipedal locomotion control based on model predictive control and divergent component of motion," *2017 IEEE International Conference on Robotics and Automation (ICRA)* 3505–3510, doi: 10.1109/ICRA.2017.7989401.
- [2] C. P. Santos, N. Alves, and J. C. Moreno, 2017, "Biped Locomotion Control through a Biomimetic CPG-based Controller," *Journal of Intelligent and Robotic Systems* 85: 47–70, doi: https://doi.org/10.1007/s10846-016-0407-3.
- [3] S. Auddy, S. Magg, and S. Wermter, 2019, "Hierarchical Control for Bipedal Locomotion using Central Pattern Generators and Neural Networks," *2019 2019 Joint IEEE 9th International Conference on Development and Learning and Epigenetic Robotics (ICDL-EpiRob)*, 13–18, doi: 10.1109/DEVLRN.2019.8850683.
- [4] M. Thor, T. Kulvicius, and P. Manoonpong, 2021, "Generic Neural Locomotion Control Framework for Legged Robots," *IEEE Transactions on Neural Networks and Learning Systems*, 32(9):doi: 10.1109/TNNLS.2020.3016523.
- [5] A. D. Myers, J. R. Tempelman, D. Petruschenko, and F. A. Khasawneh, 2020, "Low-cost double pendulum for high-quality data collection with open-source video tracking and analysis," *HardwareX*, 8: e00138, Oct. doi: 10.1016/J.OHX.2020.E00138.
- [6] T. Zielinska, G. R. R. Coba, and W. Ge, 2021, "Variable Inverted Pendulum Applied to Humanoid Motion Design," *Robotica*, 39(8): 1368–1389, doi: https://doi.org/10.1017/S0263574720001228.
- [7] A. Bahramian, F. Towhidkhal, S. Jafari, and O. Boubaker, 2020, "A double pendulum model for human walking control on the treadmill and stride-to-stride fluctuations: Control of step length, time, velocity, and position on the treadmill," *Control Theory in Biomedical Engineering*. 267–285. doi: 10.1016/B978-0-12-821350-6.00010-X.
- [8] T. Orhanli and A. Yilmaz, 2019, "Analysis of Gait Dynamics with the Double Pendulum Model," in *2019 27th Signal Processing and Communications Applications Conference (SIU)*. 1–4. doi: 10.1109/SIU.2019.8806587.
- [9] W. Ren and R. W. Beard, 2008. *Distributed Consensus in Multi-vehicle Cooperative Control*, 1st ed. London: Springer, doi: https://doi.org/10.1007/978-1-84800-015-5.
- [10] D. W. Djamari, 2020 "Distributed position estimation approach for multiagent formation with size scaling," *Asian Journal of Control* 24(1): 439-447, doi: 10.1002/asjc.2430.
- [11] Z. Lin, W. Ding, G. Yan, C. Yu, and A. Giua, "Leader-follower formation via complex Laplacian," *Automatica*, 49(6): 1900-1906, 2013, doi: 10.1016/j.automatica.2013.02.055.
- [12] M. Mesbahi and M. Egerstedt, 2010. *Graph theoretic methods in multiagent networks*. doi: 10.1515/9781400835355.
- [13] W. Ren and R. W. Beard, 2005, "Consensus seeking in multiagent systems under dynamically changing interaction topologies," *IEEE Transactions on Automatic Control*, 50(5): 655 – 661 doi: 10.1109/TAC.2005.846556.
- [14] H. G. Tanner, 2004 "On the controllability of nearest neighbor interconnections," in *Proceedings of the IEEE Conference on Decision and Control*, 3. doi: 10.1109/cdc.2004.1428782.
- [15] S. Kajita and K. Tani, 1996 "Experimental Study of Biped Dynamic Walking," *IEEE Control Systems Magazine*, 16(1): 13 – 19. doi: 10.1109/37.482132.
- [16] U.S. Department of Health and Human Services, 2018 *Physical Activity Guidelines for Americans 2nd edition*. [Online]. Available: https://health.gov/sites/default/files/2019-09/Physical\_Activity\_Guidelines\_2nd\_edition.pdf. 1 August 2022
- [17] H. K. Khalil, 2002. *Nonlinear Systems 3rd ed*, 18(16) Prentice Hall

Appendix

APPENDIX A - Derivation of Inverted Double Pendulum Model

Continuing from equation (33):

$$L = E_k - E_p \tag{A1}$$

$$E_k = \frac{1}{2}m_1(\dot{x}_1^2 + \dot{y}_1^2) + \frac{1}{2}m_2(\dot{x}_2^2 + \dot{y}_2^2)$$

$$E_k = \frac{1}{2} \left\{ m_1 [(\dot{\theta}_A l_1 \cos \theta_A)^2 + (\dot{\theta}_A l_1 \sin \theta_A)^2] \right. \\ \left. + m_2 [(\dot{\theta}_A l_1 \cos \theta_A + \dot{\theta}_B l_2 \cos \theta_B)^2 + (\dot{\theta}_A l_1 \sin \theta_A + \dot{\theta}_B l_2 \sin \theta_B)^2] \right\} \tag{A2}$$

$$E_k = \frac{1}{2} \left\{ m_1 \dot{\theta}_A^2 l_1^2 \right. \\ \left. + m_2 [(\dot{\theta}_A l_1 \cos \theta_A + \dot{\theta}_B l_2 \cos \theta_B)^2 + 2\dot{\theta}_A \dot{\theta}_B l_1 l_2 \cos \theta_A \cos \theta_B] \right. \\ \left. + m_2 [(\dot{\theta}_A l_1 \sin \theta_A + \dot{\theta}_B l_2 \sin \theta_B)^2 + 2\dot{\theta}_A \dot{\theta}_B l_1 l_2 \sin \theta_A \sin \theta_B] \right\}$$

$$E_k = \frac{1}{2} \{ m_1 \dot{\theta}_A^2 l_1^2 + m_2 \dot{\theta}_A^2 l_1^2 + m_2 \dot{\theta}_B^2 l_2^2 + 2m_2 \dot{\theta}_A \dot{\theta}_B l_1 l_2 \cos(\theta_A - \theta_B) \}$$

$$E_p = m_1 g y_1 + m_2 g y_2$$

$$E_p = m_1 g (-l_1 \cos \theta_A) + m_2 g (-l_1 \cos \theta_A - l_2 \cos \theta_B) \tag{A3}$$

For  $\theta_A$

$$\frac{d}{dt} \left( \frac{\partial L}{\partial \dot{\theta}_A} \right) - \frac{\partial L}{\partial \theta_A} = T_1 \tag{A4}$$

$$\frac{\partial L}{\partial \theta_A} = -m_2 \dot{\theta}_A \dot{\theta}_B l_1 l_2 \sin(\theta_A - \theta_B) - g l_1 \sin \theta_A (m_1 + m_2) \tag{A5}$$

$$\frac{\partial L}{\partial \dot{\theta}_A} = \frac{1}{2} \{ 2m_1 \dot{\theta}_A l_1^2 + 2m_2 \dot{\theta}_A l_1^2 + 2m_2 \dot{\theta}_B l_1 l_2 \cos(\theta_A - \theta_B) \} \tag{A6}$$

$$\frac{d}{dt} \left( \frac{\partial L}{\partial \dot{\theta}_A} \right) = \ddot{\theta}_A l_1^2 (m_1 + m_2) + \ddot{\theta}_B m_2 l_1 l_2 \cos(\theta_A - \theta_B) \\ - (\dot{\theta}_A - \dot{\theta}_B) m_2 l_1 l_2 \dot{\theta}_B \sin(\theta_A - \theta_B) \tag{A7}$$

Substituting equations (A7) and (A5) to equation (A4) we get:

$$T_1 = \ddot{\theta}_A l_1^2 (m_1 + m_2) + \ddot{\theta}_B m_2 l_1 l_2 \cos(\theta_A - \theta_B) \\ + \dot{\theta}_B^2 m_2 l_1 l_2 \sin(\theta_A - \theta_B) + g l_1 \sin \theta_A (m_1 + m_2) \tag{A8}$$

For  $\theta_B$

$$\frac{d}{dt} \left( \frac{\partial L}{\partial \dot{\theta}_B} \right) - \frac{\partial L}{\partial \theta_B} = T_1 - T_2 \tag{A9}$$

$$\frac{\partial L}{\partial \theta_B} = m_2 \dot{\theta}_A \dot{\theta}_B l_1 l_2 \sin(\theta_A - \theta_B) - m_2 g l_2 \sin \theta_B \tag{A10}$$

$$\frac{\partial L}{\partial \dot{\theta}_B} = \frac{1}{2} \{ 2m_2 \dot{\theta}_B l_1^2 + 2m_2 \dot{\theta}_A l_1 l_2 \cos(\theta_A - \theta_B) \} \tag{A11}$$

$$\frac{d}{dt} \left( \frac{\partial L}{\partial \dot{\theta}_B} \right) = \ddot{\theta}_B m_2 l_1^2 + \ddot{\theta}_A m_2 l_1 l_2 \cos(\theta_A - \theta_B) \\ - (\dot{\theta}_A - \dot{\theta}_B) m_2 l_1 l_2 \dot{\theta}_A \sin(\theta_A - \theta_B) \tag{A12}$$

Let  $T_1 - T_2 = \bar{T}_2$ , by substituting equations (A10) and (A12) to equation (A9) we get:

$$\bar{T}_2 = \ddot{\theta}_B m_2 l_1^2 + \ddot{\theta}_A m_2 l_1 l_2 \cos(\theta_A - \theta_B) \\ - \dot{\theta}_A^2 m_2 l_1 l_2 \sin(\theta_A - \theta_B) + m_2 g l_2 \sin \theta_B \tag{A13}$$

From equations (A8) and (A13) we get:

$$\ddot{\theta}_A = \frac{T_1 - \ddot{\theta}_B m_2 l_1^2 \cos(\theta_A - \theta_B) - \dot{\theta}_B^2 m_2 l_1 l_2 \sin(\theta_A - \theta_B) - g l_1 \sin \theta_A (m_1 + m_2)}{l_1^2 (m_1 + m_2)} \tag{A14}$$

$$\ddot{\theta}_B = \frac{\bar{T}_2 - \ddot{\theta}_A m_2 l_1 l_2 \cos(\theta_A - \theta_B) + \dot{\theta}_A^2 m_2 l_1 l_2 \sin(\theta_A - \theta_B) - m_2 g l_2 \sin \theta_B}{m_2 l_1^2} \tag{A15}$$

By substituting equation (A14) to equation (A13) and equation (A15) to equation (A8), and letting  $\theta_A = \theta_1$ ;  $\theta_B = \theta_3$ , also  $\theta_2 = \dot{\theta}_1$  and  $\theta_4 = \dot{\theta}_3$ , we can get the final form of the differential equation:

$$\ddot{\theta}_2 = p \left[ \frac{T_1}{l_1^2} - \frac{\bar{T}_2 \cos(\theta_1 - \theta_3)}{l_1 l_2} - \frac{\dot{\theta}_1^2 m_2 l_2 \sin(\theta_1 - \theta_3)}{l_1} - \frac{g(m_1 + m_2) \sin \theta_1}{l_1} \right]$$

$$- \left[ \frac{-\dot{\theta}_2^2 m_2 \sin(\theta_1 - \theta_3) \cos(\theta_1 - \theta_3)}{l_1} + \frac{g m_2 \sin \theta_3 \cos(\theta_1 - \theta_3)}{l_1} \right]$$

$$\ddot{\theta}_4 = p(m_1 + m_2) \left[ \frac{\bar{T}_2}{m_2 l_2^2} - \frac{T_1 \cos(\theta_1 - \theta_3)}{l_1 l_2 (m_1 + m_2)} + \frac{\dot{\theta}_1^2 l_1 \sin(\theta_1 - \theta_3)}{l_2} - \frac{g \sin \theta_3}{l_2} \right]$$

$$+ \left[ \frac{\dot{\theta}_2^2 m_2 \sin(\theta_1 - \theta_3) \cos(\theta_1 - \theta_3)}{(m_1 + m_2)} + \frac{g \sin \theta_1 \cos(\theta_1 - \theta_3)}{l_2} \right] \tag{A16}$$

where  $p = \frac{1}{m_1 + m_2 - m_2 \cos^2(\theta_1 - \theta_3)}$

APPENDIX B - Linearization of Inverted Double Pendulum Model

Following is the linearization of the double pendulum model of equation (A16):

$$\delta \ddot{\theta}_1 = \frac{\partial \ddot{\theta}_1}{\partial \theta_1} \delta \theta_1 + \frac{\partial \ddot{\theta}_1}{\partial \theta_2} \delta \theta_2 + \frac{\partial \ddot{\theta}_1}{\partial \theta_3} \delta \theta_3 + \frac{\partial \ddot{\theta}_1}{\partial \theta_4} \delta \theta_4 + \frac{\partial \ddot{\theta}_1}{\partial T_1} \delta T_1 + \frac{\partial \ddot{\theta}_1}{\partial \bar{T}_2} \delta \bar{T}_2$$

$$\delta \dot{\theta}_1 = \delta \theta_2 \tag{B1}$$

$$\delta \ddot{\theta}_2 = \frac{\partial \ddot{\theta}_2}{\partial \theta_1} \delta \theta_1 + \frac{\partial \ddot{\theta}_2}{\partial \theta_2} \delta \theta_2 + \frac{\partial \ddot{\theta}_2}{\partial \theta_3} \delta \theta_3 + \frac{\partial \ddot{\theta}_2}{\partial \theta_4} \delta \theta_4 + \frac{\partial \ddot{\theta}_2}{\partial T_1} \delta T_1 + \frac{\partial \ddot{\theta}_2}{\partial \bar{T}_2} \delta \bar{T}_2$$

$$\delta \dot{\theta}_2 = \alpha_1 \delta \theta_1 + \alpha_2 \delta \theta_2 + \alpha_3 \delta \theta_3 + \alpha_4 \delta \theta_4 + \alpha_5 \delta T_1 + \alpha_6 \delta \bar{T}_2 \tag{B2}$$

where:

$$\alpha_1 = \frac{1}{p} \left\{ \frac{-2T_1 m_2 \cos(\theta_1 - \theta_3) \sin(\theta_1 - \theta_3)}{p l_1^2} + \frac{\bar{T}_2 \sin(\theta_1 - \theta_3)}{l_1 l_2} + \frac{2T_1 m_2 \cos^2(\theta_1 - \theta_3) \sin(\theta_1 - \theta_3)}{p l_1 l_2} \right. \\ \left. + \frac{2m_2^2 l_2 \dot{\theta}_2^2 \sin^2(\theta_1 - \theta_3) \cos(\theta_1 - \theta_3)}{p l_1} + \frac{2m_2 g \sin(\theta_1 - \theta_3) \sin \theta_3 \cos(\theta_1 - \theta_3)}{p l_1} \right. \\ \left. - \frac{m_2 l_2 \dot{\theta}_1^2 \cos^2(\theta_1 - \theta_3) - g \cos \theta_1 (m_1 + m_2)}{l_1} + m_2 \dot{\theta}_2^2 (\sin^2(\theta_1 - \theta_3) - \cos^2(\theta_1 - \theta_3)) \right. \\ \left. + \frac{2m_2^2 \dot{\theta}_2^2 \sin^2(\theta_1 - \theta_3) \cos^2(\theta_1 - \theta_3)}{p} - \frac{m_2 g \sin(\theta_1 - \theta_3) \sin \theta_3}{l_1} \right. \\ \left. - \frac{2m_2^2 g \cos^2(\theta_1 - \theta_3) \sin(\theta_1 - \theta_3) \sin \theta_3}{p} \right\}$$

$$\alpha_2 = \frac{-2m_2 \dot{\theta}_2 \sin(\theta_1 - \theta_3) \cos(\theta_1 - \theta_3)}{p l_1}$$

$$\alpha_3 = \frac{1}{p} \left\{ \frac{2T_1 m_2 \cos(\theta_1 - \theta_3) \sin(\theta_1 - \theta_3)}{p l_1^2} - \frac{\bar{T}_2 \sin(\theta_1 - \theta_3)}{l_1 l_2} - \frac{2T_1 m_2 \cos^2(\theta_1 - \theta_3) \sin(\theta_1 - \theta_3)}{p l_1 l_2} \right. \\ \left. - \frac{2m_2^2 l_2 \dot{\theta}_2^2 \sin^2(\theta_1 - \theta_3) \cos(\theta_1 - \theta_3)}{p l_1} - \frac{2m_2 g \sin(\theta_1 - \theta_3) \sin \theta_3 \cos(\theta_1 - \theta_3)}{p l_1} \right. \\ \left. + \frac{m_2 l_2 \dot{\theta}_1^2 \cos^2(\theta_1 - \theta_3)}{l_1} + \frac{m_2 g \cos(\theta_1 - \theta_3) \cos \theta_3}{l_1} + \frac{m_2 g \sin(\theta_1 - \theta_3) \sin \theta_3}{l_1} \right. \\ \left. + \frac{2m_2^2 g \cos^2(\theta_1 - \theta_3) \sin(\theta_1 - \theta_3) \sin \theta_3}{l_1} - \frac{2m_2 g \cos(\theta_1 - \theta_3) \sin(\theta_1 - \theta_3) \sin \theta_3 (m_1 + m_2)}{p} \right. \\ \left. + m_2 \dot{\theta}_2^2 (\cos^2(\theta_1 - \theta_3) - \sin^2(\theta_1 - \theta_3)) - \frac{2m_2^2 \dot{\theta}_2^2 \sin^2(\theta_1 - \theta_3) \cos^2(\theta_1 - \theta_3)}{p} \right\}$$

$$\alpha_4 = \frac{-2m_2 l_2 \dot{\theta}_4 \sin(\theta_1 - \theta_3)}{p l_1}$$

$$\alpha_5 = \frac{1}{p l_1^2}$$

$$\alpha_6 = \frac{-\cos(\theta_1 - \theta_3)}{p l_1 l_2}$$

$$\delta \ddot{\theta}_3 = \frac{\partial \ddot{\theta}_3}{\partial \theta_1} \delta \theta_1 + \frac{\partial \ddot{\theta}_3}{\partial \theta_2} \delta \theta_2 + \frac{\partial \ddot{\theta}_3}{\partial \theta_3} \delta \theta_3 + \frac{\partial \ddot{\theta}_3}{\partial \theta_4} \delta \theta_4 + \frac{\partial \ddot{\theta}_3}{\partial T_1} \delta T_1 + \frac{\partial \ddot{\theta}_3}{\partial \bar{T}_2} \delta \bar{T}_2$$

$$\delta \dot{\theta}_3 = \delta \theta_4 \tag{B3}$$

$$\delta \ddot{\theta}_4 = \frac{\partial \ddot{\theta}_4}{\partial \theta_1} \delta \theta_1 + \frac{\partial \ddot{\theta}_4}{\partial \theta_2} \delta \theta_2 + \frac{\partial \ddot{\theta}_4}{\partial \theta_3} \delta \theta_3 + \frac{\partial \ddot{\theta}_4}{\partial \theta_4} \delta \theta_4 + \frac{\partial \ddot{\theta}_4}{\partial T_1} \delta T_1 + \frac{\partial \ddot{\theta}_4}{\partial \bar{T}_2} \delta \bar{T}_2$$

$$\delta \dot{\theta}_4 = b_1 \delta \theta_1 + b_2 \delta \theta_2 + b_3 \delta \theta_3 + b_4 \delta \theta_4 + b_5 \delta T_1 + b_6 \delta \bar{T}_2 \tag{B4}$$

where:

$$b_1 = \frac{1}{p} \left\{ \frac{-2T_1 (m_1 + m_2) \cos(\theta_1 - \theta_3) \sin(\theta_1 - \theta_3)}{p l_2^2} + \frac{T_1 \sin(\theta_1 - \theta_3)}{l_1 l_2} + \frac{2T_1 m_2 \cos^2(\theta_1 - \theta_3) \sin(\theta_1 - \theta_3)}{p l_1 l_2} \right. \\ \left. + \frac{2m_2 (m_1 + m_2) g \sin(\theta_1 - \theta_3) \sin \theta_3 \cos(\theta_1 - \theta_3)}{p l_2} + \frac{(m_1 + m_2) l_1 \dot{\theta}_2^2 \cos(\theta_1 - \theta_3)}{l_2} \right. \\ \left. - \frac{2m_2 (m_1 + m_2) l_1 \dot{\theta}_2^2 \sin^2(\theta_1 - \theta_3) \cos(\theta_1 - \theta_3)}{p l_2} + m_2 \dot{\theta}_4^2 (\cos^2(\theta_1 - \theta_3) - \sin^2(\theta_1 - \theta_3)) \right. \\ \left. - \frac{2m_2^2 \dot{\theta}_4^2 \cos^2(\theta_1 - \theta_3) \sin^2(\theta_1 - \theta_3)}{p} + \frac{(m_1 + m_2) g \cos(\theta_1 - \theta_3) \cos \theta_3}{l_2} \right. \\ \left. - \frac{(m_1 + m_2) g \sin(\theta_1 - \theta_3) \sin \theta_3}{l_2} - \frac{2m_2 (m_1 + m_2) \cos^2(\theta_1 - \theta_3) \sin(\theta_1 - \theta_3) \sin \theta_3}{p l_2} \right\}$$

$$b_2 = \frac{-2(m_1 + m_2) l_1 \dot{\theta}_2 \sin(\theta_1 - \theta_3)}{p l_2}$$

$$b_3 = \frac{1}{p} \left\{ \frac{2T_1 (m_1 + m_2) \cos(\theta_1 - \theta_3) \sin(\theta_1 - \theta_3)}{p l_2^2} - \frac{T_1 \sin(\theta_1 - \theta_3)}{l_1 l_2} - \frac{2T_1 m_2 \cos^2(\theta_1 - \theta_3) \sin(\theta_1 - \theta_3)}{p l_1 l_2} \right. \\ \left. + \frac{2m_2 (m_1 + m_2) l_1 \dot{\theta}_2^2 \sin^2(\theta_1 - \theta_3) \cos(\theta_1 - \theta_3)}{p l_2} - \frac{(m_1 + m_2) l_1 \dot{\theta}_2^2 \cos(\theta_1 - \theta_3)}{l_2} \right. \\ \left. - \frac{(m_1 + m_2) g \cos \theta_3}{l_2} - \frac{2m_2 (m_1 + m_2) g \cos(\theta_1 - \theta_3) \cos(\theta_1 - \theta_3) \sin(\theta_1 - \theta_3) \sin \theta_3}{p l_2} \right. \\ \left. + \frac{m_2 \dot{\theta}_4^2 (\sin^2(\theta_1 - \theta_3) - \cos^2(\theta_1 - \theta_3))}{p} + \frac{2m_2 \dot{\theta}_4^2 \sin^2(\theta_1 - \theta_3) \cos^2(\theta_1 - \theta_3)}{p} \right. \\ \left. + \frac{(m_1 + m_2) g \sin(\theta_1 - \theta_3) \sin \theta_3}{l_2} + \frac{2m_2 (m_1 + m_2) g \cos^2(\theta_1 - \theta_3) \sin(\theta_1 - \theta_3) \sin \theta_3}{p l_2} \right\}$$

$$b_4 = \frac{2m_2 \dot{\theta}_4 \cos(\theta_1 - \theta_3) \sin(\theta_1 - \theta_3)}{p}$$

$$b_5 = \frac{-\cos(\theta_1 - \theta_3)}{l_1 l_2 p}$$

$$b_6 = \frac{(m_1 + m_2)}{m_2 l_2^2 p}$$